remote sensing

MDPI

Communication

New Evidence to Support Zephyria Tholus as a Composite Volcano on Mars

Le Wang [1,†], Jiannan Zhao [1,†], Jun Huang [1,2,*] and Long Xiao [1]

[1] State Key Laboratory of Geological Processes and Mineral Resources, Planetary Science Institute, School of Earth Sciences, China University of Geosciences, Wuhan 430074, China; lewang@cug.edu.cn (L.W.); jnzhao@cug.edu.cn (J.Z.); longxiao@cug.edu.cn (L.X.)
[2] Chinese Academy of Sciences Center for Excellence in Comparative Planetology, Hefei 230026, China
* Correspondence: junhuang@cug.edu.cn
† The authors contribute equally.

Abstract: Zephyria Tholus has been proposed to be a composite volcano, however, detailed geomorphological study was not carried out due to limited high-resolution remote sensing data. Here we use MOLA, THEMIS, CTX and HiRISE data to conduct topographical and geomorphological analysis of Zephyria Tholus. We identify extensive valleys and troughs on the flank, which are sector collapse or glacio-fluvial in origin. The valleys and troughs indicate coexistence of different erosion resistance materials, along with the observed solid lava outcrops. There are also layered materials identified on the wall of the largest valley. In addition, perched craters are identified on the top depression and flanks of Zephyria Tholus, indicating the presence of ice-rich layer. We conducted crater size-frequency distribution of the caldera and found the absolute model age is 3.74 (+0.03, −0.04) Ga. The geomorphology evidence and chronology result support the composite volcano nature of Zephyria Tholus, and indicate the magma volatile content in the Aeolis region in Noachian is more than 0.15 wt% if the atmosphere paleo-pressure was similar to present Mars.

Keywords: composite volcano; remote sensing; Mars

Citation: Wang, L.; Zhao, J.; Huang, J.; Xiao, L. New Evidence to Support Zephyria Tholus as a Composite Volcano on Mars. *Remote Sens.* **2021**, *13*, 3891. https://doi.org/10.3390/rs13193891

Academic Editors: Lin Li, Yuanzhi Zhang and Shengbo Chen

Received: 29 August 2021
Accepted: 21 September 2021
Published: 28 September 2021

1. Introduction

Mars has a long history of volcanism [1,2]. Various volcanic landforms have been identified since the Mariner 9 and Viking data [3,4]. Large shield volcanoes in the Tharsis and Elysium volcanic province show geomorphological characteristics of low-viscosity effusive basaltic lavas (e.g., [5]), while large ash shields lying in Circum-Hellas region are inferred to form by friable materials [4,6–8]. It has been proposed that explosive eruption was dominated in early Mars geological history [9,10], and effusive eruption dominated later [11]. The transition of explosive and effusive eruption generates composite volcanoes. Therefore, extensive composite volcanoes should have existed on Mars. Olympus Mons and Alba Patera have been proposed to have explosive eruptions in their early history [12,13]; however, the geological evidence has been buried or erased by subsequent processes. Zephyria Tholus, lying in the Aeolis region, was hypothesized to be a composite volcano [14], but spatial coverage and resolution of the remote sensing data hindered detailed characterization of this edifice. Here, we carry out geomorphological study of Zephyria Tholus with recently acquired imaging data and provide constraints on its volcanic activities. The results support the composite volcano nature of Zephyria Tholus. It provides clues into the transition of volcanic eruption style and the volatile contents in the magma on Mars.

2. Methods

We use Mars Orbiter Laser Altimeter (MOLA: 128 ppd) [15] Precision Experiment Data Record (PEDR) to extract topographical profile and calculate slopes of Zephyria Tholus.

MOLA Mission Experiment Gridded Data Record (MEGDR) was used to visualize the regional topography. Thermal Emission Imaging System (THEMIS: [16]) global mosaic (~100 m/pixel) [17] provides regional geomorphological context of the surface materials. We use Context Camera (CTX) [18] global mosaic (~6 m/pixel) [19] and images of High Resolution Imaging Science Experiment (HiRISE ~25–30 cm/pixel) [20] to characterize the detailed geomorphological features. To study the topography of small-scale features, we build CTX Digital Terran Model (DTM) from CTX stereo pairs using NASA Ames Stereo Pipeline [21]. We carry out crater size-frequency distribution (CSFD) measurements on CTX global mosaic with ArcGIS plugin Cratertools [22], and analyze the CSFD data with Craterstats2 [23].

3. Results

Zephyria Tholus (Figure 1a), centered at ~19.8°S, 172.94°E, lies in the Aeolis region of Mars. This cone-shaped feature is ~350 km away from the center of Gusev crater, and the adjacent has been mapped as the Early Noachian Highland (eNh) unit [10]. Zephyria Tholus rises ~3 km with a basal diameter of ~30 km. The southern flank is steeper than the north, and the maximum slopes is 20° (Figure 1b). The flanks of the feature are heavily etched with extensive valleys and channels (Figure 2a). No lava flow lobes have been identified on the flank nor the surrounding area. There is a depression on the top of Zephyria Tholus with a diameter of ~8.4 km, and it slightly tilts to the north (Figure 1b). The surface of the depression is covered by air fall dust, which makes spectral mineral identification very challenging.

3.1. Age

We studied the size-frequency distribution of craters larger than 60 m in diameter to estimate the model age of the caldera. The product function is adopted from [24], and the chronology function is from [25]. The absolute model age derived is 3.74 (+0.03, −0.04) Ga (Figure 2b), which falls in the Noachian period. This age is consistent with the previously mapped eNh unit [10] of the region. The real age is likely to be older than the derived absolute model age due to the coverage of airfall dust. The absolute model age of the caldera indicated that the Zephyria Tholus stopped volcanic eruption in the Late Noachian.

3.2. Geomorphology Features

3.2.1. Valleys, Planèzes and Channels

We have identified 7 obvious valleys on the north and west flanks (Figure 2a), the longest one is ~15 km in length and up to 120 m in depth, and the widths of the valleys are 2–4 km. The volume of materials removed from the valleys is ~1–13 km^3. The cross-sectional profiles of the valleys display "V" shapes (Figure 2c). Two of the valleys are relatively large, extends from Zephyria Tholus summit to its base, and the other valleys located near the base. We also identified 11 channels radially distributed on the flanks of Zephyria Tholus (Figure 2a). Additionally, we identified 4 planes (Figure 2a), which is a triangular facet on the flanks of a conical feature [26]. Planes are formed by radial drainage systems and they are the remnants of the original surface of volcanoes [27].

3.2.2. Layered Materials

We have identified layered materials on the wall of the largest valley on Zephyria Tholus' flank, and air-fall dust covering the rest area (Figure 3b). Large numbers of boulders up to 1.5 m diameter are observed ~500 m to 1000 m away from the layered materials (Figure 3d). The boulders are likely from the layered materials and survived from movement, indicating that the layered materials are solid rocks in nature [11].

3.2.3. Perched Craters

We identify craters with radial ejecta on the flanks and caldera (Figure 3e,f) with available HiRISE images (PSP_004032_1600 and ESP_016743_1600). The diameters of this

type of craters are typically less than 50 m. Interestingly, the ejecta looks elevated in topography even at the distal end. These craters are similar to previously reported perched craters [28], which indicates the existence of ice while the impact event occurred. The ejecta protected the ice from sublimation. The distribution of the perched craters on the surface of Zephyria Tholus likely has bias due to the limited coverage of HiRISE data.

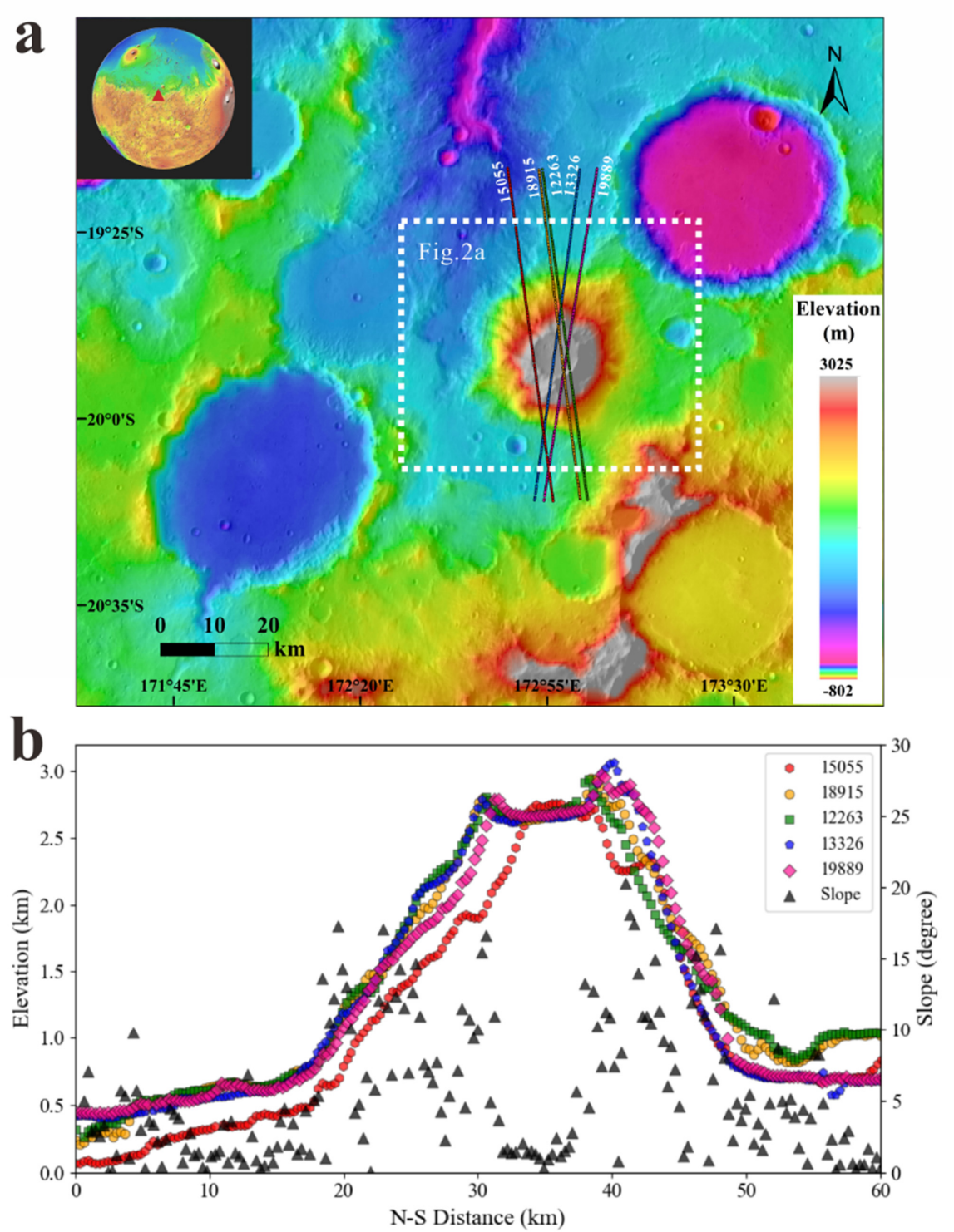

Figure 1. (**a**) Regional context of Zephyria Tholus. The volcano lies in the Early Noachian terrain. The image is color-coded MOLA MEGDR over THEMIS day IR mosaic [15,16]. MOLA PEDR footprints (tracks 15,055, 18,915, 12,263, 13,326 and 19,889) over Zephyria Tholus are indicated with dots. (**b**) Elevation profiles (10 times vertical exaggeration) extracted from MOLA PEDR. The slopes are calculated from PEDR track 12,263 with a baseline of 0.3 km.

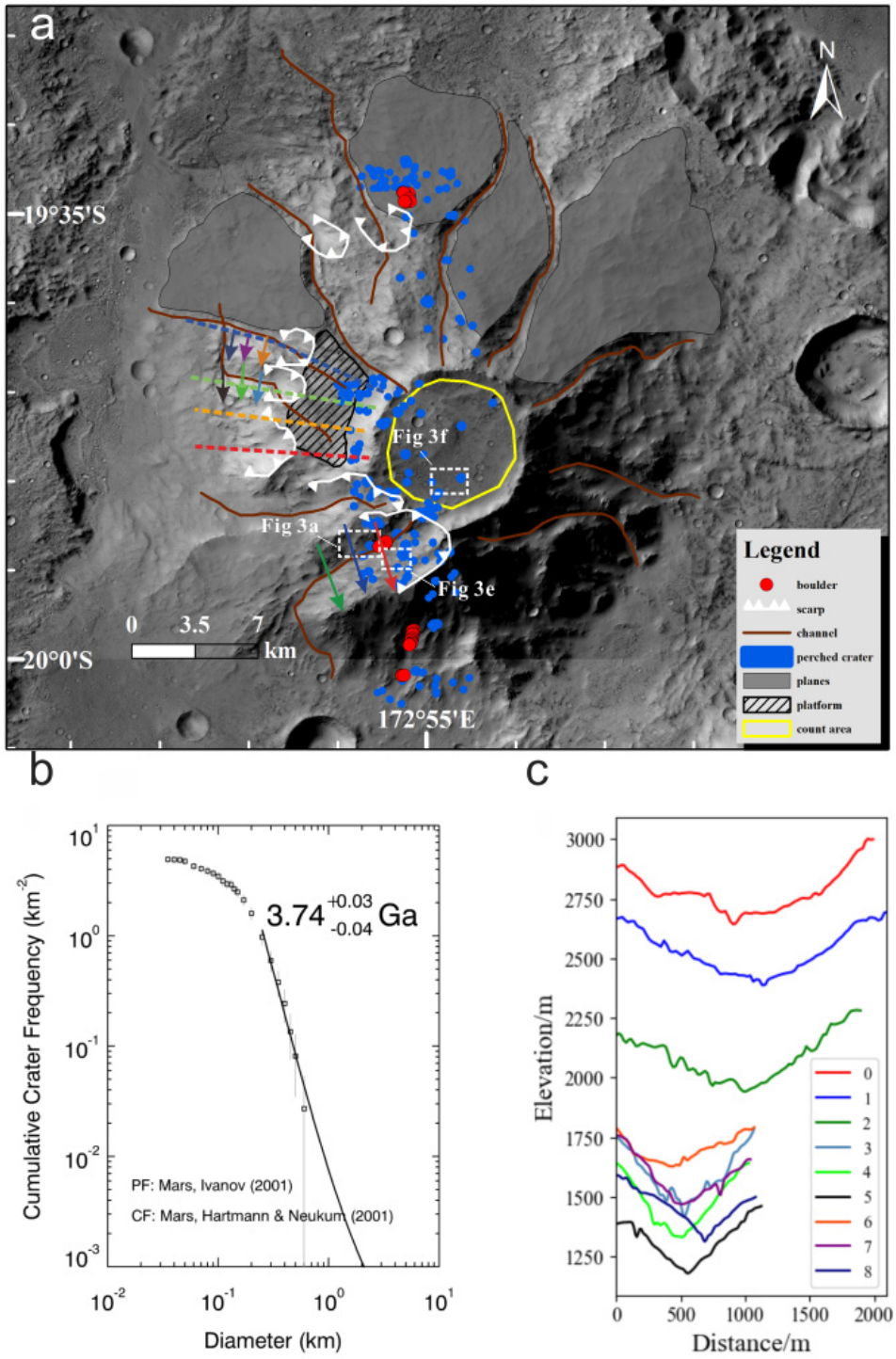

Figure 2. (**a**) Geomorphological characteristics of Zephyria Tholus. Crescentic scarps at the top of the valleys are indicated by white lines with ticks facing downwards. Color lines with arrows indicate the location of the extracted topographical cross sections. The yellow solid line delineates the area for crater size-frequency distribution measurements. Blue polygons indicate the locations of perched craters and the red dots indicate boulders. Color dash lines represent the profile tracks of Figure 4. Brown solid lines represent the channels. The image is CTX global mosaic [19]. (**b**) The cumulative crater size-frequency distribution and absolute model age of the Zephyria Tholus caldera. (**c**) Cross-sectional profiles of the three valleys on the flank. Elevation data are extracted from CTX DTM, which is generated from the stereo pair of CTX images B18_016743_1597_XI_20S187W and P15_006801_1609_XI_19S187W.

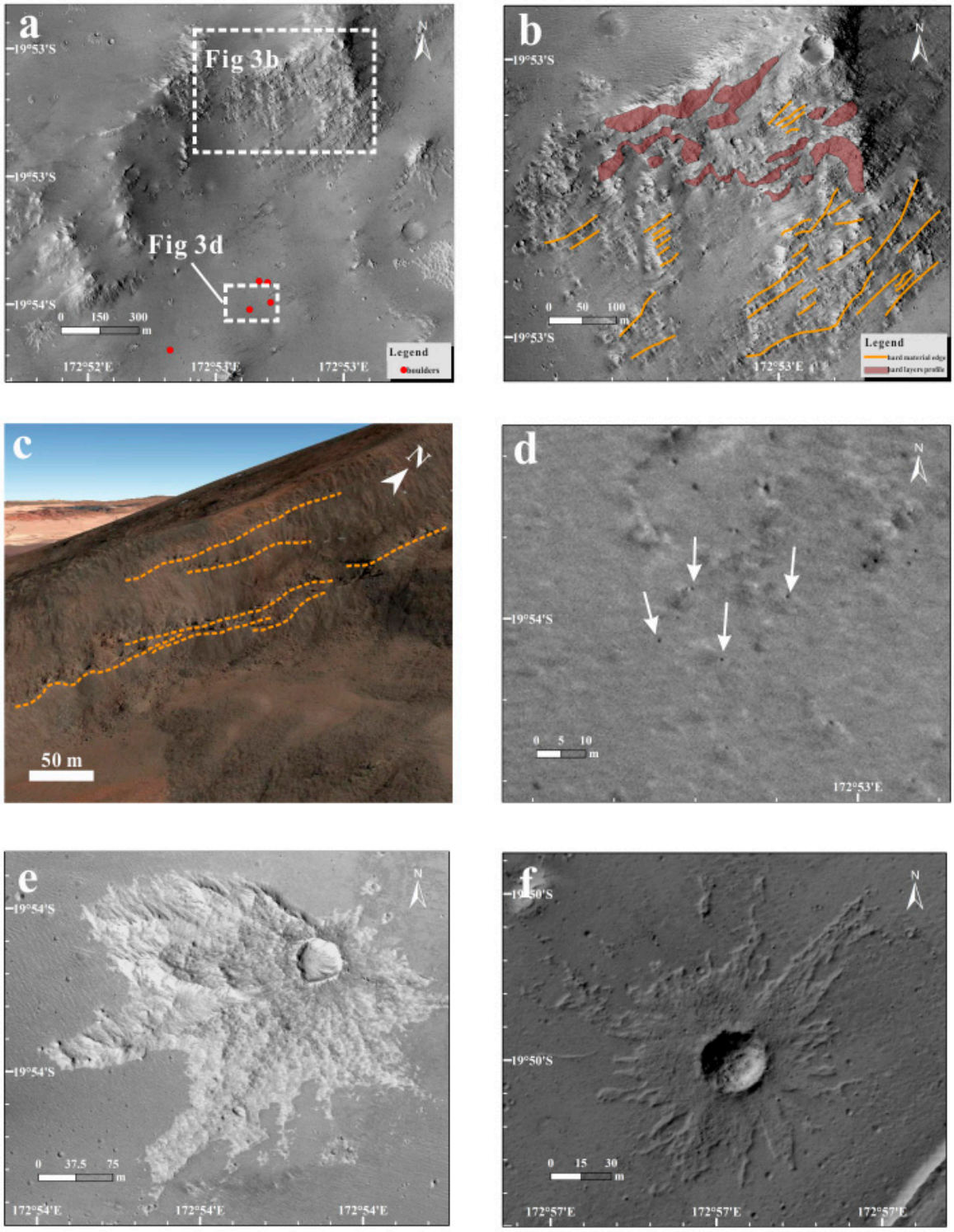

Figure 3. (**a**) The overview diagram of layered materials and boulders. The boulders are marked with red dots and they are ~500 to 1000 m away from the layered materials. Portion of HiRISE image PSP_004032_1600_RED. (**b**) Layered materials exposed on the wall of a valley on the flank of Zephyria Tholus. The thickness of the layer is ~100 m. Color polygons represent the profile and orange solid lines are the edge of hard material. (**c**) An oblique view of the wall of an amphitheater-shaped hollow on the flank of a composite volcano, Palpana volcano in the Atacama Desert of Chile. Orange dash lines represent the layered material. The image is from Google Earth. (**d**) The identified boulders are indicated by white arrows. (**e**) A perched crater on the flank. Asymmetric ejecta is observed. (**a**,**b**,**d**,**e**) are all the portion of HiRISE image PSP_004032_1600_RED. (**f**) A perched crater on the surface of the caldera. The ejecta surface looks relatively smooth. Portion of HiRISE image ESP_016743_1600_RED.

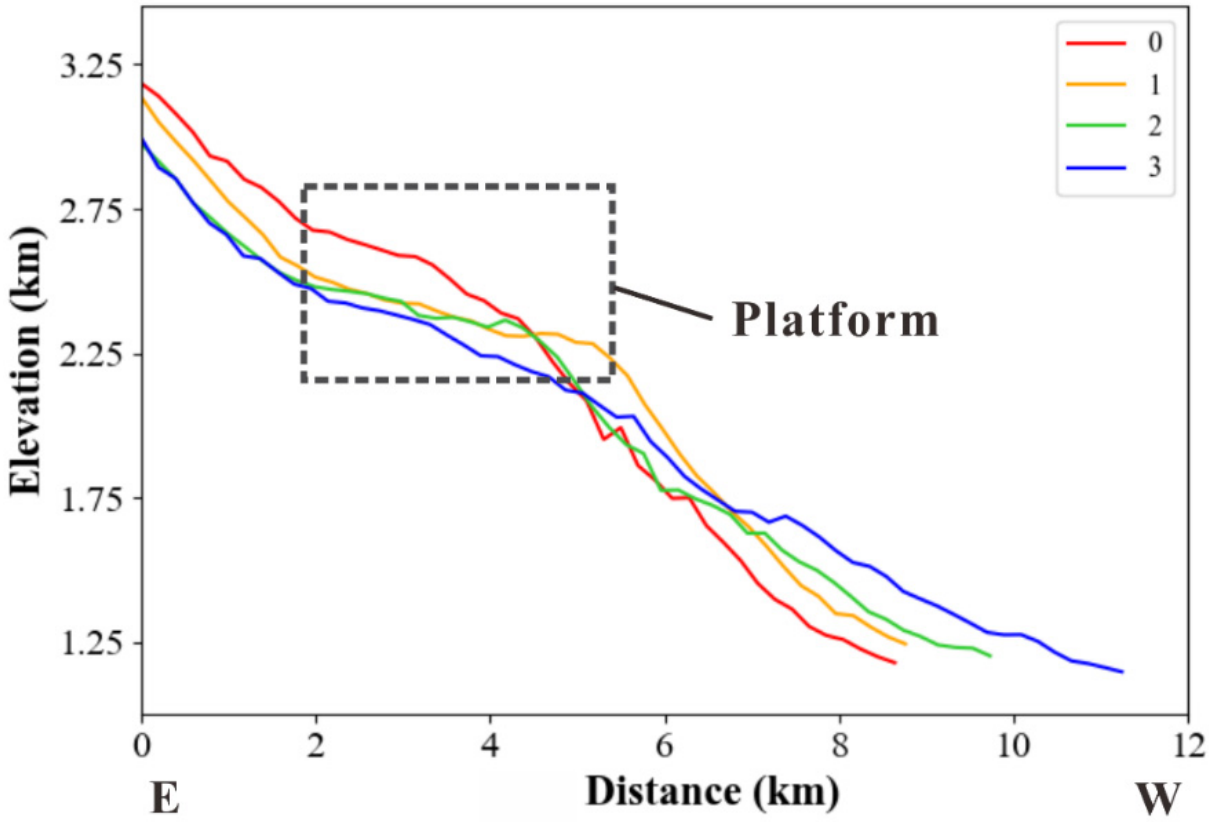

Figure 4. The topographic profile indicates the presence of gentle slope region on the west flank of Zephyria Tholus. The elevation with 4 times exaggeration was extracted from CTX DEM.

4. Discussion

Zephyria Tholus was hypothesized to be a composite volcano due to elevated slope comparing to the slopes of other shield volcanoes on Mars [14,29]. Stewart and Head (2001) proposed four causes of Zephyria Tholus: (1) stacking of multiple crater edges; (2) cliffs produced by faults or other structures; (3) volcanic construction; and (4) differential erosion. The cone shape, lack of surrounding marginal stacking impact craters and absence of previously existing faulting and differential-weathering of similar structures, indicate the volcanic origin of Zephyria Tholus. On Earth, the denudation history of the composite volcano is divided into five stages, in which the fourth stage is characterized by virtually invisible lava flows, deep river valleys, large planes, primitive conical surfaces with extensive modification, prominent topographic protrusions, and U-shaped valleys formed by glacial erosion [26]. The geomorphic characteristics observed on the surface Zephyria Tholus are consistent with the fourth stage of erosion of terrestrial composite volcanoes. We calculated the volume of Zephyria Tholus, which is about 744 km^3. The volumes is comparable to terrestrial composite volcanoes, whose volumes vary from 10 to 1000 km^3 [30].

On Earth, the slope of composite volcanoes can reach up to 35°; however, the maximum slope of Zephyria Tholus is ~20° (Figure 1b). On Mars, where gravity is lower than on Earth, lava flows with same composition could flow farther across the surface than on Earth. When magma viscosity and velocity are the same, the height of a volcano is inversely proportional to the radius of its undersurface [31]. As the distance of the lava flow increases, the radius of the base of the volcano becomes larger, the height that the volcano could grow to decreases, and the slope becomes slower. The erosion of the surface reduced the height of Zephyria Tholus, which in turn decreased its slope.

We have investigated the Palpana volcano (21.54°S, 68.52°W) in the Atacama Desert of Chile. The climate of this area is very arid and similar to the present environment of Mars. The Palpana volcano is a composite volcano (stratovolcano) [32], with the height of 2.02 km and slope of 26° [33]. There is a large amphitheater-shaped hollow (Figure 5a) on its southern flank, which is formed by glacial erosion [34]. The morphological characters are extremely similar to Zephyria Tholus. There are also some layered materials on the wall of the hollow (Figure 3c), which are the lava flows in multiple periods [32]. We also identified similar structures on the valley wall of Zephyria Tholus. The similarity in geomorphology between Zephyria Tholus and the Palpana volcano indicates similar origin and subsequent modification.

Composite volcanoes are built with alternant effusive and explosive eruptions. The fine-material layers between solid lava layers are relatively weak (Figure 3b), and they increase instability during magma intrusion or hydrothermal activity [35]. The extensive valleys observed on the flank of Zephyria Tholus formed from erosion by sector collapse or glacio-fluvial activities. The variations in length and width of valleys indicate different mechanisms of formation. The valleys developed near the lower flank are likely to form from sector collapse, or erosion by ice-melting water. Sector collapse is a structure formed by instability within the volcano, allowing parts of the flank to collapse and slide down the foothills, often resulting in a steepening of the volcanic flank, which is easier to develop in a composite volcano [35]. It is indicated by crescentic scarps (Figure 2a), which bend towards downslope. The slider moves along the flank to form the slump bulge at the basal of the scarps, and there usually developed gully along the side of the slider [35]. However, the slide is likely removed by subsequent modification. The alternative formation mechanism is erosion by ice-melting water. It can be seen from the topographic profile that there is a portion with a gentle slope above the valley on the west wing (Figure 4). After the ice melted and water flooded, the surface collapses and forms a platform. The glacio-fluvial formation mechanism for the valleys on the lower part of Zephyria Tholus is preferred due to the ice-related features mentioned above and the absence of evident observations for magmatic intrusion or hydrothermal action.

The wide occurrence of perched craters (Figures 2a and 3e,f) on the surface of Zephyria Tholus suggests the existence of ice-rich materials. This leads to the hypothesis that glacial process may involve in the formation of the lager valleys. In addition, the morphology of the valley heads on the flank is similar to cirques (Figure 5b,c) developed on the Popocatepetl volcano in Central Mexico [36]. A cirque is an amphitheater-like concave topography created by glacial erosion, and it opens to the downhill side. The bottom of a cirque is usually flat. However, we identified V-shaped cross-sectional profiles for the valleys (Figure 2c), which indicates fluvial activities are essential in the formation of these valleys.

It is difficult to distinguish the formation mechanism of the valleys on the flank of Zephyria Tholus from different scenarios. However, no matter they are formed by sector collapse or glacio-fluvial erosion, flank materials composed of erosion-resistant layers and interlaced easily eroded layers are needed. The coexistence of different strength materials indicates alternating deposits of pyroclastic materials and solid lava, which strongly supports that Zephyria Tholus is a composite volcano in nature.

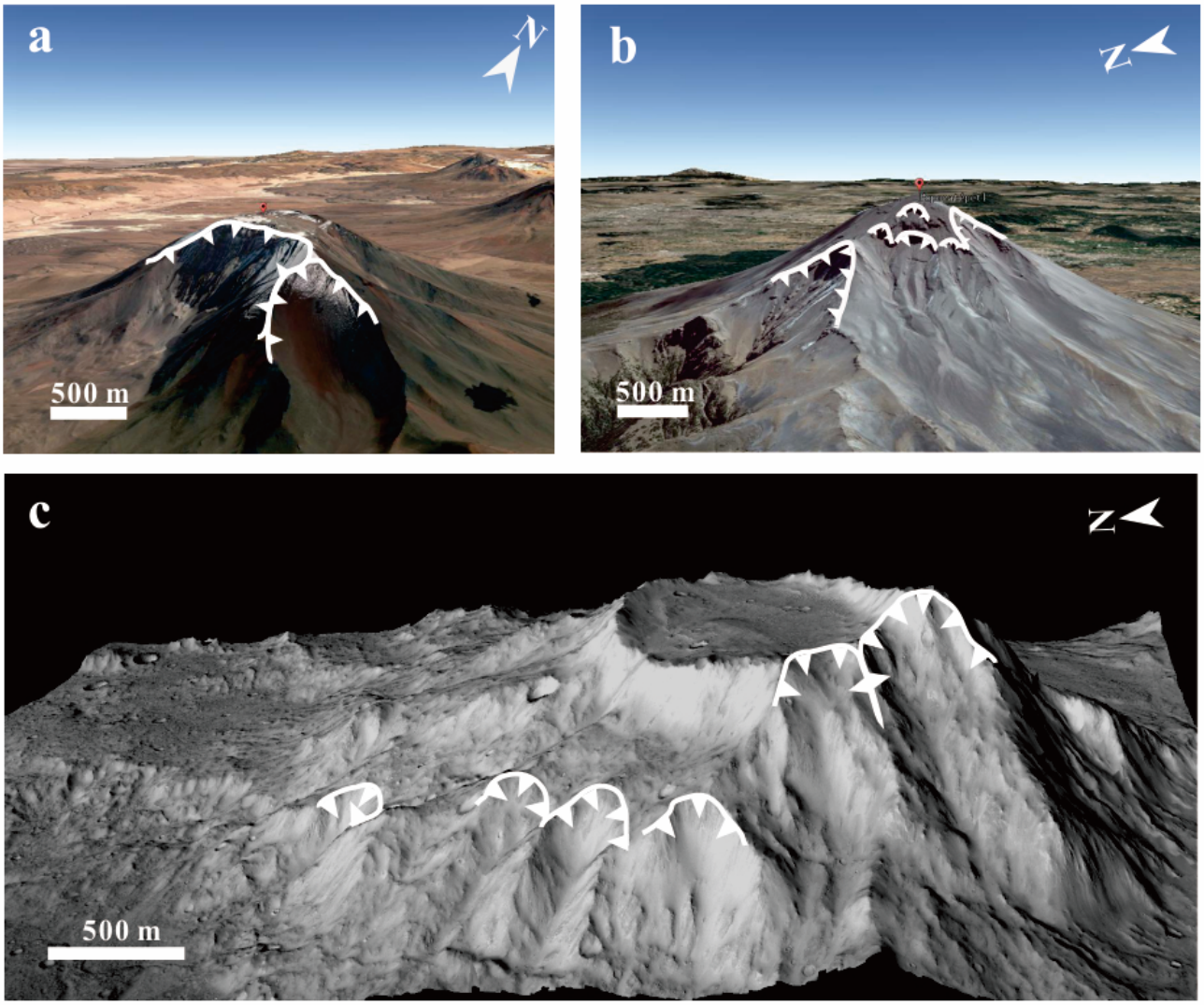

Figure 5. A couple of cirques on Popocatepetl volcano, amphitheater-shaped hollow on Palpana volcano and a series of valleys on the flank of Zephyria Tholus. (**a**) An oblique view of Palpana volcano. White lines represent the scarps of the amphitheater-shaped hollows. The image if from Google Earth. (**b**) An oblique view of Popocatepetl volcano. The white line indicates the scarp at the top of a cirque. The image is from Google Earth. (**c**) An oblique view of Zephyria Tholus. The white lines show the crescentic scarps at the heads of the valleys. The image is CTX global mosaic [19] on 3-time exaggeration CTX DEM.

Volcanism on Mars started with globally distributed center vents and fissures ~4.0 Ga ago and centralized to Tharsis, Elysium and Circus-Hellas provinces [1,2,37]. The dominant volcanic eruption style changes from explosive to effusive [9,11,38]. More composite volcanoes should have formed early in Mars' history, however, they are buried by later volcanism or modified by other subsequent geological processes. Zephyria Tholus is the most possible candidate composite volcano so far. If this is confirmed, it will provide key insights into volcanism and paleoclimate in Noachian. Explosive eruption is driven by volatiles in the magma or in the environment. The gravity of Mars is lower than on Earth, so the depth of nucleation of volatiles and subsequent disruption of magma is larger on Mars. With current Martian surface atmospheric pressure and the effect of altitude, Hawaiian-style eruption could happen with magma volatile content larger than 0.03 wt% in the region of Tharsis; basaltic Pliny eruptions require 0.2% versus 0.15% volatiles [39]. The elevation of Aeolis region is much lower than that of Tharsis region, and the atmospheric pressure is relatively large. In the case of Zephyria Tholus as a composite volcano, the volatile content required for explosive eruption may be even higher

than 0.15 wt%. Previous study shows that 99% of the atmosphere had been lost before ~3.8 Ga [40]. The absolute model age of the Zephyria Tholus caldera is ~3.74 Ga, therefore, the solid lava (Figure 3b) indicates the volatiles in the magma were more than 0.15 wt% in the Late Noachian to the Early Hesperian. The eruption type of a volcano is not only related to the volatile content, but also to the viscosity and temperature of the magma. On Earth, low-viscosity magma (10–10^4 Pa s) is favorable to the efficient segregation of gas bubbles and ductile melt deformation [41]. In the end, a relatively quiet Hawaiian eruption or a strombolian eruption, and explosive eruption is not likely to occur. The formation of explosive volcanoes is due to the higher vapor pressure of the magma than confining pressure of the surrounding rock and atmospheric pressure. During the eruption, a large amount of gas carrying pyroclastic materials and volcanic ash is ejected from the crater. Due to low atmospheric pressure, fragmentation of basaltic magma or interaction between magma and groundwater, Plinian eruptions are relatively common on Mars [42]. Therefore, if the magma that formed Zephyria Tholus was basaltic, the volatile content of the magma was at least 0.15 wt%, and even more volatile could be accumulated when the magma was of high viscosity as it prevents the segregation of gas bubbles from magma. At present, we cannot determine the nature of the magma that formed Zephyria Tholus, but we believe that the volatile content of the magma in the Aeolis region was greater than 0.15 wt%.

5. Conclusions

Zephyria Tholus is a composite volcano on Mars from topography and geomorphology evidence using recently acquired high-resolution orbital data. Zephyria Tholus provides important clues on the magma volatiles in the Noachian, thus it is a good candidate for future in situ exploration.

Author Contributions: Conceptualization, J.H.; methodology, L.W. and J.Z.; writing—original draft preparation, L.W., J.Z. and J.H.; writing—review and editing, L.W., J.Z., J.H. and L.X.; visualization, L.W. and J.Z.; funding acquisition, J.H. All authors have read and agreed to the published version of the manuscript.

Funding: This research was funded by the Strategic Priority Research Program of the Chinese Academy of Sciences (XDB 41000000), the National Natural Science Foundation of China (41773061, 42002305, 41830214), the Pre-research Project on Civil Aerospace Technologies of CNSA (D020101).

Institutional Review Board Statement: Not applicable.

Informed Consent Statement: Not applicable.

Data Availability Statement: The MOLA, CTX and HiRISE data are achieved in the PDS Geosciences Node (https://ode.rsl.wustl.edu/mars/, accessed on 14 December 2020). The THEMIS data is achieved in the ASU Mars Space Flight Facility Node (http://www.mars.asu.edu/, accessed on 14 December 2020).

Acknowledgments: We gratefully acknowledge Planetary Data System archive for providing the MOLA, CTX, HiRISE and THEMIS data. The review by James Head at an earlier stage of the manuscript greatly improved the quality. We thank three anonymous referees for their constructive suggestions.

Conflicts of Interest: The authors declare no conflict of interest.

References

1. Werner, S.C. The global martian volcanic evolutionary history. *Icarus* **2009**, *201*, 44–68. [CrossRef]
2. Xiao, L.; Huang, J.; Christensen, P.R.; Greeley, R.; Williams, D.A.; Zhao, J.; He, Q. Ancient volcanism and its implication for thermal evolution of Mars. *Earth Planet. Sci. Lett.* **2012**, *323*, 9–18. [CrossRef]
3. Carr, M.H. Volcanism on mars. *J. Geophys. Res.* **1973**, *78*, 4049–4062. [CrossRef]
4. Greeley, R.; Spudis, P.D. Volcanism on mars. *Rev. Geophys.* **1981**, *19*, 13–41. [CrossRef]
5. Zimbelman, J.; Garry, W.; Bleacher, J.; Crown, D. Volcanism on Mars. In *The Encyclopedia of Volcanoes*; Academic Press: Cambridge, MA, USA, 2015; Chapter 41.
6. Peterson, J. Volcanism in the Noachis-Hellas region of Mars, 2. In Proceedings of the Lunar and Planetary Science Conference Proceedings, Houston, TX, USA, 13–17 March 1978; pp. 3411–3432.

7. Williams, D.A.; Greeley, R.; Zuschneid, W.; Werner, S.C.; Neukum, G.; Crown, D.A.; Gregg, T.K.; Gwinner, K.; Raitala, J. Hadriaca Patera: Insights into its volcanic history from Mars express high resolution stereo camera. *J. Geophys. Res. Planets* **2007**, *112*, E10. [CrossRef]
8. Williams, D.A.; Greeley, R.; Werner, S.C.; Michael, G.; Crown, D.A.; Neukum, G.; Raitala, J. Tyrrhena Patera: Geologic history derived from Mars express high resolution stereo camera. *J. Geophys. Res. Planets* **2008**, *113*, E11. [CrossRef]
9. Huang, J.; Xiao, L. Knobby terrain on ancient volcanoes as an indication of dominant early explosive volcanism on Mars. *Geophys. Res. Lett.* **2014**, *41*, 7019–7024. [CrossRef]
10. Tanaka, K.L.; Skinner, J.A., Jr.; Dohm, J.M.; Irwin, R.P., III; Kolb, E.J.; Fortezzo, C.M.; Platz, T.; Michael, G.G.; Hare, T.M. Geologic Map of Mars. 2014. Available online: https://pubs.usgs.gov/sim/3292/ (accessed on 11 December 2020).
11. Bandfield, J.L.; Edwards, C.S.; Montgomery, D.R.; Brand, B.D. The dual nature of the martian crust: Young lavas and old clastic materials. *Icarus* **2013**, *222*, 188–199. [CrossRef]
12. King, J.S.; Riehle, J.R. A proposed origin of the Olympus Mons escarpment. *Icarus* **1974**, *23*, 300–317. [CrossRef]
13. Mouginis-Mark, P.; Wilson, L.; Zimbelman, J.R. Polygenic eruptions on Alba Patera, Mars. *Bull. Volcanol.* **1988**, *50*, 361–379. [CrossRef]
14. Stewart, E.M.; Head, J.W. Ancient Martian volcanoes in the Aeolis region: New evidence from MOLA data. *J. Geophys. Res. Planets* **2001**, *106*, 17505–17513. [CrossRef]
15. Smith, D.E.; Zuber, M.T.; Frey, H.V.; Garvin, J.B.; Head, J.W.; Muhleman, D.O.; Pettengill, G.H.; Phillips, R.J.; Solomon, S.C.; Zwally, H.J. Mars Orbiter Laser Altimeter: Experiment summary after the first year of global mapping of Mars. *J. Geophys. Res. Planets* **2001**, *106*, 23689–23722. [CrossRef]
16. Christensen, P.R.; Jakosky, B.M.; Kieffer, H.H.; Malin, M.C.; McSween, H.Y.; Nealson, K.; Mehall, G.L.; Silverman, S.H.; Ferry, S.; Caplinger, M. The thermal emission imaging system (THEMIS) for the Mars 2001 Odyssey Mission. *Space Sci. Rev.* **2004**, *110*, 85–130. [CrossRef]
17. Edwards, C.; Nowicki, K.; Christensen, P.; Hill, J.; Gorelick, N.; Murray, K. Mosaicking of global planetary image datasets: 1. Techniques and data processing for Thermal Emission Imaging System (THEMIS) multi-spectral data. *J. Geophys. Res. Planets* **2011**, *116*, E10. [CrossRef]
18. Malin, M.C.; Bell, J.F.; Cantor, B.A.; Caplinger, M.A.; Calvin, W.M.; Clancy, R.T.; Edgett, K.S.; Edwards, L.; Haberle, R.M.; James, P.B. Context camera investigation on board the Mars Reconnaissance Orbiter. *J. Geophys. Res. Planets* **2007**, *112*, E5. [CrossRef]
19. Dickson, J.; Kerber, L.; Fassett, C.; Ehlmann, B. A global, blended CTX mosaic of Mars with vectorized seam mapping: A new mosaicking pipeline using principles of non-destructive image editing. In Proceedings of the Lunar and planetary science conference, The Woodlands, TX, USA, 19–23 March 2018; pp. 1–2.
20. McEwen, A.S.; Eliason, E.M.; Bergstrom, J.W.; Bridges, N.T.; Hansen, C.J.; Delamere, W.A.; Grant, J.A.; Gulick, V.C.; Herkenhoff, K.E.; Keszthelyi, L. Mars reconnaissance orbiter's high resolution imaging science experiment (HiRISE). *J. Geophys. Res. Planets* **2007**, *112*, E5. [CrossRef]
21. Shean, D.E.; Alexandrov, O.; Moratto, Z.M.; Smith, B.E.; Joughin, I.R.; Porter, C.; Morin, P. An automated, open-source pipeline for mass production of digital elevation models (DEMs) from very-high-resolution commercial stereo satellite imagery. *ISPRS J. Photogramm. Remote Sens.* **2016**, *116*, 101–117. [CrossRef]
22. Kneissl, T.; van Gasselt, S.; Neukum, G. Map-projection-independent crater size-frequency determination in GIS environments—New software tool for ArcGIS. *Planet. Space Sci.* **2011**, *59*, 1243–1254. [CrossRef]
23. Michael, G.; Neukum, G. Surface dating: Software tool for analysing crater size-frequency distributions including those showing partial resurfacing events. In Proceedings of the Lunar and Planetary Science Conference, League City, TX, USA, 10–14 March 2008; p. 1780.
24. Ivanov, B.A. Mars/Moon cratering rate ratio estimates. *Space Sci. Rev.* **2001**, *96*, 87–104. [CrossRef]
25. Neukum, G.; Ivanov, B.A.; Hartmann, W.K. Cratering records in the inner solar system in relation to the lunar reference system. *Chronol. Evol. Mars* **2001**, *96*, 55–86. [CrossRef]
26. Davidson, J.; De Silva, S. Composite volcanoes. *Encycl. Volcanoes* **2000**, *1*, 663–681.
27. Ollier, C.; Terry, J. Volcanic geomorphology of northern Viti Levu, Fiji. *Aust. J. Earth Sci.* **1999**, *46*, 515–522. [CrossRef]
28. Kadish, S.J.; Head, J.W. Impacts into non-polar ice-rich paleodeposits on Mars: Excess ejecta craters, perched craters and pedestal craters as clues to Amazonian climate history. *Icarus* **2011**, *215*, 34–46. [CrossRef]
29. Plescia, J. Morphometric properties of Martian volcanoes. *J. Geophys. Res. Planets* **2004**, *109*, E3. [CrossRef]
30. de Silva, S.; Lindsay, J.M. Primary volcanic landforms. In *The Encyclopedia of Volcanoes*; Elsevier: Amsterdam, The Netherlands, 2015; pp. 273–297.
31. Lacey, A.; Ockendon, J.; Turcotte, D. On the geometrical form of volcanoes. *Earth Planet. Sci. Lett.* **1981**, *54*, 139–143. [CrossRef]
32. Wörner, G.; Hammerschmidt, K.; Henjes-Kunst, F.; Lezaun, J.; Wilke, H. Geochronology (40Ar/39Ar, K-Ar and He-exposure ages) of Cenozoic magmatic rocks from northern Chile (18-22 S): Implications for magmatism and tectonic evolution of the central Andes. *Rev. Geológica De Chile* **2000**, *27*, 205–240.
33. Francis, P.; Wells, G. Landsat Thematic Mapper observations of debris avalanche deposits in the Central Andes. *Bull. Volcanol.* **1988**, *50*, 258–278. [CrossRef]
34. Francis, P.; De Silva, S. Application of the Landsat Thematic Mapper to the identification of potentially active volcanoes in the Central Andes. *Remote Sens. Environ.* **1989**, *28*, 245–255. [CrossRef]

35. de Vries, B.v.W.; Kerle, N.; Petley, D. Sector collapse forming at Casita volcano, Nicaragua. *Geology* **2000**, *28*, 167–170. [CrossRef]
36. Espinasa-Pereña, R.; Pozzo, A. Morphostratigraphic evolution of Popocatépetl volcano, México. *Spec. Pap.-Geol. Soc. Am.* **2006**, *402*, 115.
37. Robbins, S.J.; Di Achille, G.; Hynek, B.M. The volcanic history of Mars: High-resolution crater-based studies of the calderas of 20 volcanoes. *Icarus* **2011**, *211*, 1179–1203. [CrossRef]
38. Brož, P.; Bernhardt, H.; Conway, S.J.; Parekh, R. An overview of explosive volcanism on Mars. *J. Volcanol. Geotherm. Res.* **2020**, *409*, 107125. [CrossRef]
39. Head, J.W.; Wilson, L. Tharsis Montes as composite volcanoes? The role of explosive volcanism in edifice construction and implications for the volatile contents of edifice-forming magmas. In Proceedings of the Lunar and Planetary Science Conference, Houston, TX, USA, 16–20 March 1998; p. 1127.
40. Catling, D.C. Atmospheric Evolution, Mars. In *Encyclopedia of Paleoclimatology and Ancient Environments*; Gornitz, V., Ed.; Springer: Dordrecht, The Netherlands, 2009; pp. 66–75.
41. Taddeucci, J.; Edmonds, M.; Houghton, B.; James, M.R.; Vergniolle, S. Hawaiian and Strombolian eruptions. In *The encyclopedia of Volcanoes*; Elsevier: Amsterdam, The Netherlands, 2015; pp. 485–503.
42. Wilson, L.; Head, J.W., III. Mars: Review and analysis of volcanic eruption theory and relationships to observed landforms. *Rev. Geophys.* **1994**, *32*, 221–263. [CrossRef]